

# A98-31564

ICAS-98-3,9,1

## STUDY OF ENVIRONMENT EFFECTS BY MEANS OF SCALE MODEL FLIGHT TESTS IN A LABORATORY

Patricia COTON  
ONERA/DCSD

5 Bd Paul PAINLEVE, 59000 LILLE, FRANCE

### Abstract

For the purpose of studying aerodynamics and aircraft behaviour in the low-speed domain, the Department for System Control and Flight Dynamics of ONERA (ONERA/DCSD) has developed over many years a specific experimental method based on flight tests of scale models performed in a laboratory. This method, specially used for the characterization and modelling of the handling qualities of aircraft flying in adverse environmental conditions, is particularly well adapted to the study of non-steady phenomena.

This paper first describes the facility and the main aspects of the experimental technique. The second part is relative to the modelling concepts specially developed to represent dynamic and non-steady aerodynamic effects. These concepts are presented through some applications of the experimental technique. These applications are respectively relative to flight in atmospheric turbulence, static, dynamic and non-steady ground effects and near and far-field characterization of aircraft wake vortices.

Concurrently to these studies, the project of a new laboratory is investigated to open the experimental technique to new fields of research and specially to study of new control systems and validation of control laws. The main outlines of this new laboratory project are presented by way of conclusion.

### Nomenclature

$l$	reference wing chord
$\alpha$	angle of attack
$\beta$	sideslip angle
$\gamma$	path angle
$\theta$	pitch angle
$V$	aircraft speed
$V_z$	vertical aircraft speed
$x, y, z$	body reference frame
$h$	altitude
$u, v, w$	linear velocity components in the body reference frame
$v_{gust}, w_{gust}$	gust velocity components in the body reference frame

$p, q, r$	angular rate components in the body reference frame
$C_x, C_y, C_z$	respectively drag, lateral force and lift coefficients in the air-trajectory reference frame
$C_l, C_m, C_n$	respectively rolling moment, pitching moment and yawing moment coefficients in the body reference frame
$h_F$	vertical distance between the centre of gravity and the fin's aerodynamic centre
$l_F$	horizontal distance between the centre of gravity and the fin's aerodynamic centre
$C_y \beta'$	dimensionless derivative coefficient relative to element $i$

### Introduction

With the aim of improving flight accuracy and safety, ONERA/DCSD carries out a lot of research work, relative to behaviour of aircraft at low speed under extreme flight conditions, by means of its original facilities and especially its Flight Analysis Laboratory. These extreme flight conditions are, in particular, due to atmospheric turbulence, wake disturbances and ground effects during take-off and landing phases.

To foresee and control aircraft behaviour in such adverse environmental conditions, it is necessary to have both an accurate representation of the aerodynamic efforts acting on the aircraft and a realistic representation of the disturbance itself.

What are needed here are representative models « useful » from a flight mechanics point of view and well adapted to real-time simulation. These models are essential for flight quality and performance calculation, control law design or configuration optimization and flight safety assessment.

This leads to develop specific modelling concepts to represent non-steady and transient aerodynamic effects. Examples of these concepts are :

- space-time representation with separate elements, local torques and local time lags associated with these elements,

- specific filters to represent transient effects,

and are presented here through some applications of the experimental technique.

### Experimental technique

This experimental technique<sup>(1)</sup> is based on the use of unmotorized launched models.

The model is accelerated by means of a pneumatic catapult whose height and slope angle have been previously adjusted. Once the model is launched, it flies freely without any wall or mounting interference in a 30m long, 9m wide and 10m high observation area. On the general sketch of the facility, shown in figure 1, one can distinguish the catapult, which propels the model, the evolution zone and the recovery system.

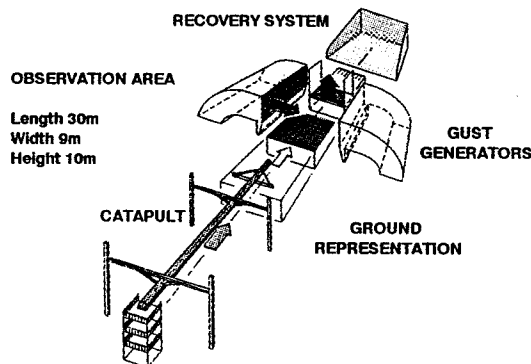


FIGURE 1 - Flight Analysis Laboratory

The initial path angle, velocity, angle of attack and sideslip angle are adjustable. Flights can be performed in still air or in a disturbed environment : lateral or vertical gusts of wind with different profiles can be introduced along the path of the model by means of wind tunnels. A floor can also be installed in the facility for ground effect studies. All these tests can be performed with or without an internal control loop.

The tests are carried out according to the Froude similarity rules which keep the ratio of the inertial forces to the gravity forces constant. This implies that all the parameters describing the phenomena will be expressed by means of the primary independent quantities (i. e. the reference length  $L$ , the air density  $\rho$  and the gravity acceleration  $g$ ).

Let  $e$  be the geometric scale of the model and  $n$  the ratio of the air densities (altitude of the aircraft flight / altitude  $Z = 0$  of the model flight). The similitude ratio of the principal physical quantities connected to the

trajectory of the plane are then presented in the table hereafter.

Quantity	Model	Aircraft
Linear acceleration	$\gamma_m$	$\gamma_m$
Linear velocity	$V_m$	$e^{1/2}V_m$
Length	$L_m$	$eL_m$
Angular rate	$\dot{\theta}_m$	$e^{-1/2}\dot{\theta}_m$
Angle	$\theta_m$	$\theta_m$
Time	$T_m$	$e^{1/2}T_m$
Mass	$m_m$	$ne^3m_m$
Inertia	$I_m$	$ne^5I_m$
Force	$F_m$	$ne^3F_m$
Moment	$M_m$	$ne^4M_m$

FIGURE 2 - Froude similitude

The basic in-board equipment is composed of some accelerometers and gyrometers, a PCM\* encoder (30 channels, 12 bit words, scanning frequency = 520Hz per channel) and static memories for data storage.

\*Pulse Code Modulation

According to the kind of tests that are to be performed, this equipment can be complemented by a pressure probe which gives information about the angle of attack, the sideslip angle and the dynamic pressure. A micro-processor to elaborate the control laws and actuators to move the control surfaces can also be added to this equipment.

The in-board information are supplemented by ground-based measurements. A velocity measurement device gives the initial velocity of the flight. Four optical bases implemented all along the evolution area of the model, each of them constituted by two cameras, enable to obtain the Euler angles and position of the centre of gravity of the model at four well-known moments of the flight. The synchronization of the information coming from the ground with the measurements coming from the model is realized by activating a photocell on the model, by means of flashlights connected with each optical base.

The trajectory and the different flight parameters (linear and angular accelerations, linear and angular velocities, ...) are then obtained through a coherence study between the data from the in-board equipment and the information from the ground. The global aerodynamic efforts are determined from these

parameters and the model inertial characteristics (mass and moments of inertia), which have been previously measured.

The span of the models is generally of the order of 1m (combat aircraft) or 2m (transport aircraft). Their mass is about 20kg and their initial velocity between 20 and 40m/s. In these conditions the Reynolds number for the tests (relatively to the mean aerodynamic wing chord) is about  $3 \cdot 10^5$  for a transport aircraft and  $3 \cdot 10^6$  for a combat aircraft.

This experimental technique offers :

- a realistic representation of aircraft behaviour and of involved phenomena (no mounting or wall interference, well-known environment),
- flight test data obtained through redundant measurements which enables us to perform an optimal valuation of the state variables and aerodynamic coefficients,
- a complementarity with low-speed wind tunnel tests, by performing realistic unsteady tests with the ability to specify the contribution of particular elements of the aircraft (horizontal tail, fin, ...) to the aerodynamic efforts and moments,
- the access to near-field and far-field characteristics of the flow round the aircraft.

Analysis and modelling of the response of an aircraft to a short gust of wind

Loads induced by a gust of long length  $L_{gust} //$  (where  $L_{gust}$  is the gust length to attain its maximum) are ordinarily considered to be the result of a change in angle of attack and sideslip angle due to the components of gust velocity at right angles to the flight path. Added changes in the rotation rates are also introduced to represent gust velocity distribution considered to be of a linear-ramp shape along the body frame of the aircraft .

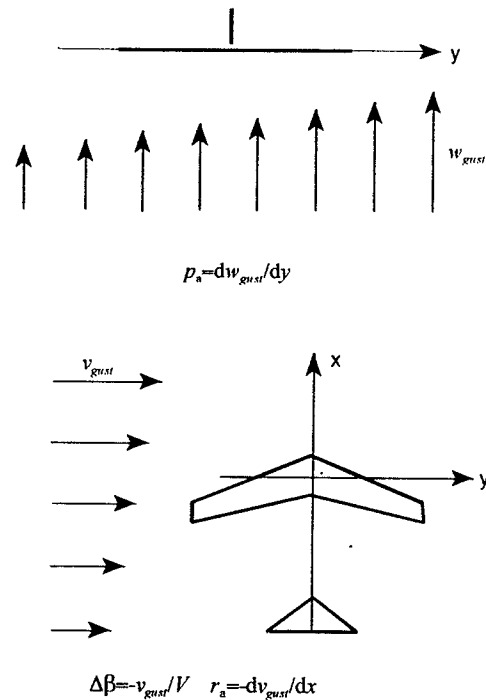
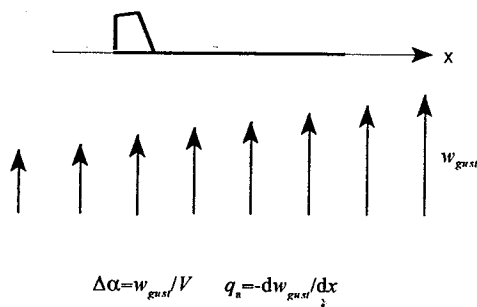


FIGURE 3 : Classical modelling for long gust effects

When the frequencies contained in the disturbance get higher, this approach is no longer valid. It is, in particular, necessary to take into account the effects due to the penetration into gust as well as the transient effects connected to the establishment of aerodynamic forces on the lifting surfaces.

The first step of the process leading to the development of a realistic modelling of these effects is to perform tests and gather experimental data describing the involved phenomena. This experimental data base is made up of scale model flight tests.

The work presented here is relative to a delta wing combat aircraft considered as a rigid aircraft. The encountered disturbance is created by a lateral wind tunnel whose independent units enable to generate gusts over various lengths. These gusts, whose profiles are adjustable by a pressure loss system, are identified before performing the test by means of hot wire measurements. The basic in-board equipment of the scale model, described in chapter 2, is complemented by an internal balance to measure the local aerodynamic forces acting on the fin. Flight parameters and global aerodynamic efforts are determined from the in-board accelerometric and gyrometric information and the ground-based measurements, associated with the inertial characteristics of the model. An example of results is presented in the figure below.

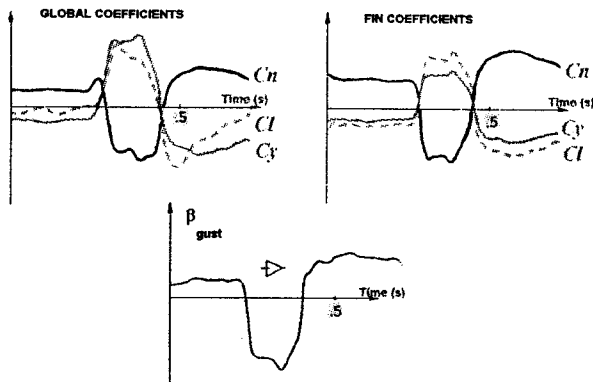


FIGURE 4 - Example of results

When the aircraft penetrates into the left-to-right gust, the disturbance acting on the forward part of the fuselage produces a small lateral force and a nose-right yawing movement. To take into account these effects, due to the penetration into the sharp edge of the gust, the aircraft is considered as a three element system :

- two elements for the fuselage and the wing, which are represented by two points T1 and T2, located on both sides of the centre of gravity,
- one element for the fin, which representative point F is its aerodynamic centre.

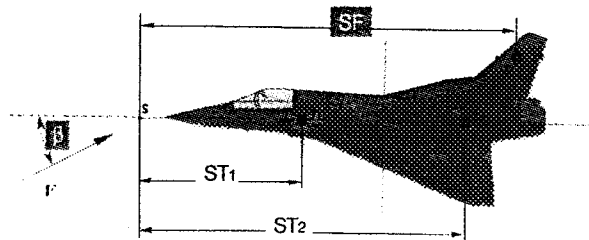


FIGURE 5 - Modelling principle

The transient effects connected to the establishment of the aerodynamic efforts are apparent on the figure below :

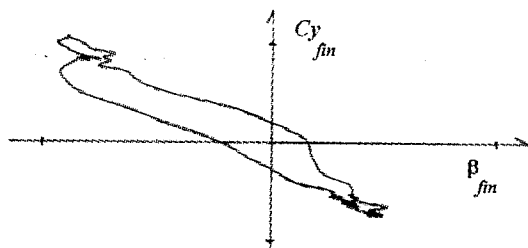


FIGURE 6 : Transient effects

$$\text{where } \beta_{fin} = \frac{v}{V} + p \frac{h_F}{V} - r \frac{l_F}{V} + \beta_{gust} \left( t - \frac{SF}{V} \right)$$

and  $\beta_{gust}(t)$  is the quantity  $-\frac{v_{gust}}{V}$  measured at point S by the probe.

These transient effects are taken into account by the way of a transfert function  $H(t)$  and this leads to the following equations for the lateral coefficients :

$$C_y = C_y^0 + \sum_{i=1}^2 C_y \beta^i \left( \beta + \beta_{gust} \left( t - \frac{ST_i}{V} \right) \right) + C_y \beta^{fin} \left( \beta + \int_0^\infty H(\tau) \beta_{gust} \left( t - \frac{SF}{V} - \tau \right) d\tau \right) + C_{yp} \frac{pl}{V} + C_{yr} \frac{rl}{V}$$

$$C_l = C_l^0 + \sum_{i=1}^2 C_l \beta^i \left( \beta + \beta_{gust} \left( t - \frac{ST_i}{V} \right) \right) + C_l \beta^{fin} \left( \beta + \int_0^\infty H(\tau) \beta_{gust} \left( t - \frac{SF}{V} - \tau \right) d\tau \right) + C_{lp} \frac{pl}{V} + C_{lr} \frac{rl}{V}$$

$$C_n = C_n^0 + \sum_{i=1}^2 C_n \beta^i \left( \beta + \beta_{gust} \left( t - \frac{ST_i}{V} \right) \right) + C_n \beta^{fin} \left( \beta + \int_0^\infty H(\tau) \beta_{gust} \left( t - \frac{SF}{V} - \tau \right) d\tau \right) + C_{np} \frac{pl}{V} + C_{nr} \frac{rl}{V}$$

where  $\beta$  is related to the components  $u, v$  et  $w$  of the speed of the center of gravity with respect to the ground,

$$\beta = \text{Arctg} \frac{v}{\sqrt{u^2 + w^2}},$$

The position of the fin aerodynamic centre and the fin static coefficients  $C_y \beta^{fin}, C_l \beta^{fin}, C_n \beta^{fin}$  are determined through static tests performed in a wind tunnel. The fuselage coefficients  $C_y \beta^i, C_l \beta^i, C_n \beta^i$  and the characteristics of the filter applied to  $\beta_{gust} \left( t - \frac{SF}{V} \right)$  are obtained through model flight tests.

Characterization and modelling of static and dynamic ground effects

Optimization of the approach and landing procedures requires identification of the aerodynamic interaction effects between aircraft and ground. These effects are of three types :

- static ground effect, corresponding to level flight close to a ground without discontinuity,
- dynamic ground effect, relative to a sink rate during the roundoff phase or to a pitch rate,
- non-steady ground effect, corresponding to flight near a discontinuous ground (deck landing for instance).

These three types of ground effects can be studied in the Flight Analysis Laboratory. The runway is represented by a floor which is installed along the path of the scale model on all or part of the available length, depending on the test to be performed. To test the static ground effect, the slope of the floor is equal to the path angle of the model flight, so that the altitude of the flight above the ground remains constant. To study the effect of a sink rate, the slope of the floor is fixed to a value different from the path angle of the flight (figure 7a). Discontinuities can also be created to represent both realistic flight conditions (deck landing) as well as stimuli corresponding to qualified mathematical inputs (doublets, steps, etc.) (figure 7b).

figure 7a

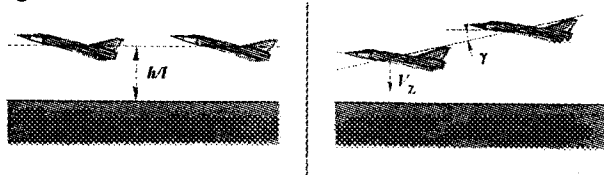


figure 7b

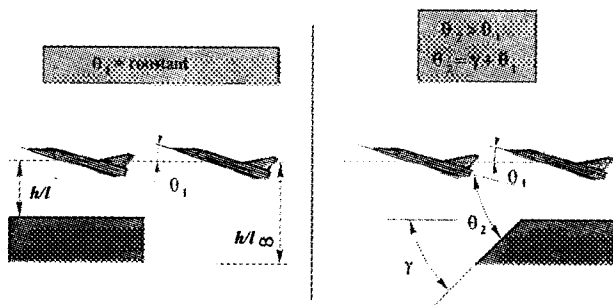


FIGURE 7 : Floor configurations

The study presented here is relative to a delta-wing combat aircraft<sup>(2)</sup>. The main characteristics of the flights which have been performed are :

- reference flights without ground effect,
- flights with continuous ground effect at various relative heights of the model over the floor,
- and flights over a discontinuous floor to study non-steady aerodynamic effects.

Figure 8 below presents an example of the relative increase in the global lift coefficient for two flights performed over a continuous floor. On this figure  $\Delta C_z$  is the difference between the lift coefficient with ground effect and the lift coefficient corresponding to the same flight parameters but without ground effect.

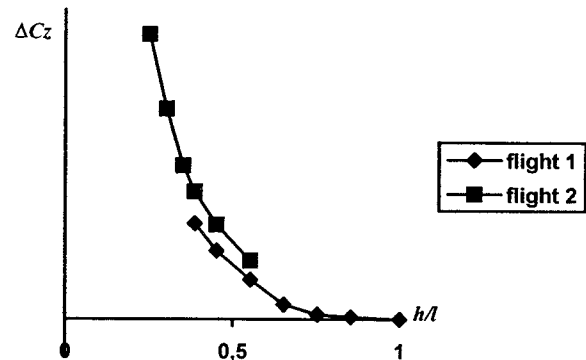


FIGURE 8 : Continuous ground effect on lift coefficient

An empirical formulation of the ground effect on the coefficients  $C_i, i = x, z, m$  has been developed from the data base made up of the tests performed over a continuous ground. This formulation takes into account the relative height of the flight over the ground and the sink rate.

$$C_{i, steady} = \alpha \left( C + \frac{A}{\left(\frac{h}{l}\right)^2} + \frac{B}{\left(\frac{h}{l}\right)} + \frac{D \frac{V_z}{V}}{\left(\frac{h}{l}\right)} \right) + \left( G + \frac{E}{\left(\frac{h}{l}\right)^2} + \frac{F}{\left(\frac{h}{l}\right)} \right)$$

for  $\frac{h}{l} \leq 0.8$

$A, B, C, D, E, F, G$  are constant and are identified from the whole data base.

To quantify the non-steady aerodynamic effects due to a rapid variation of the altitude of the aircraft over the ground, the above formulation has been compared to flight tests performed over a discontinuous floor. These conditions are encountered in particular during take-offs and landings from an aircraft carrier. These conditions are also attractive as mathematical inputs for research on general ground effect models and specially for analysis of transient effects and determination of time delays.

In the example given below (figure 9) there is no ground effect on the beginning of the flight, then the relative height of the scale model over the floor decreases abruptly down to 0.35 on a distance of 2 chords and then increases by 0.20 on a distance of 13 chords.

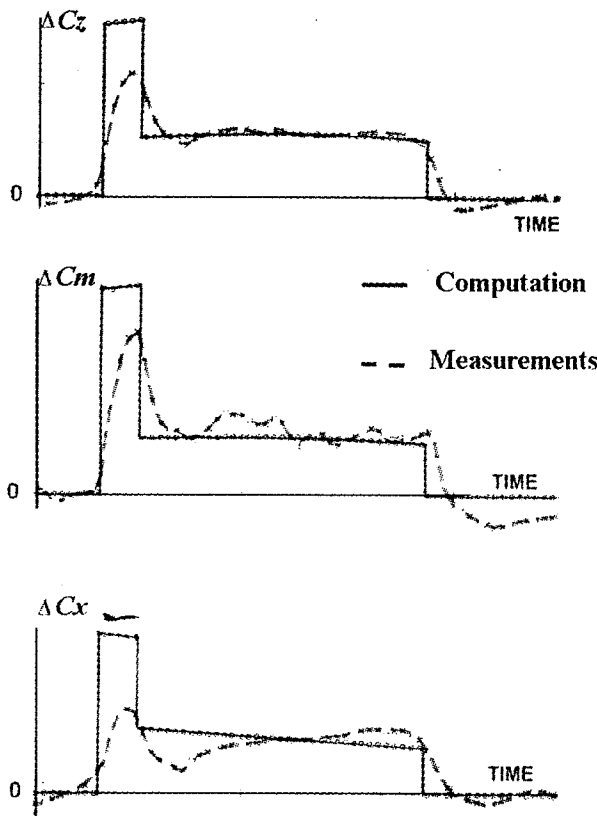


FIGURE 9 : Non-steady ground effect

On this figure  $\Delta C_i$  is the difference between the coefficient  $C_i$  with ground effect and the coefficient  $C_i$  corresponding to the same flight parameters but without ground effect. As can be seen, non-steady

ground effects are important, especially during penetration phases.

These non-steady effects are taken into account by means of transfert functions  $H(t)$  of second order, whose characteristics are depending on the sign of the floor height variation (non similar effects according to whether the aircraft goes into or out of ground effect).

$$C_{i_{steady}}(t) = \alpha(t) \left( C + \frac{A}{\left(\frac{h(t)}{l}\right)^2} + \frac{B}{\left(\frac{h(t)}{l}\right)} + \frac{D \frac{V_z(t)}{V}}{\left(\frac{h(t)}{l}\right)} \right) + \left( G + \frac{E}{\left(\frac{h(t)}{l}\right)^2} + \frac{F}{\left(\frac{h(t)}{l}\right)} \right)$$

$$C_{i_{non-steady}} = \int_0^{\infty} H(\tau) C_{i_{steady}}(t-\tau) d\tau$$

for  $i = x, z, m$

#### Characterization and modelling of transport aircraft wake

A new field of application has opened recently to the scale model flight test technique with the study of aircraft wake vortices and their impact on following aircraft<sup>(3)</sup>. Supplementing wind tunnels, this experimental method enables the observation of the wake turbulence for its whole duration (formation, evolution and decay) included with particular environmental conditions like lateral wind and ground effect.

The observations of the wake vortices, generated by the scale model, are carried out in a ground-fixed frame. Two sorts of tests are performed: smoke visualizations and measurements of local velocity by tracking or P.I.V. (Particles images velocimetry).

Smoke visualizations give information about the number of vortices with are created by a given wing configuration, the trajectory and velocity of their centres and the way they interact.

A smoke sheet, lit with a laser or with a white light produced by spotlights, is created in a plane perpendicular to the ground. Shooting is performed with a black-and-white C.C.D. video camera located under the catapult. The frequency of this video camera is equal to 50 frames (512 x 256 pixels) per second.

figure 10 a



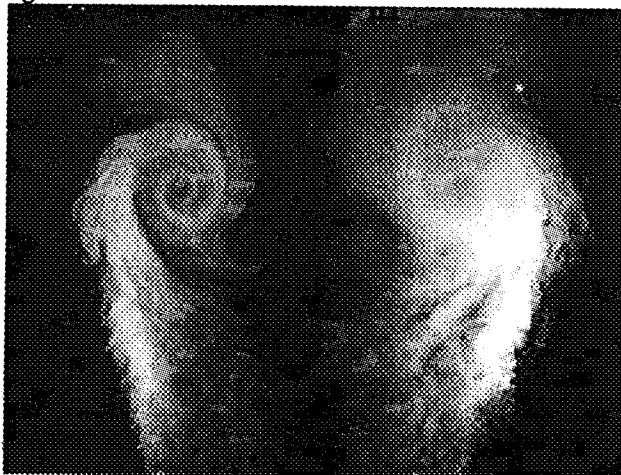
the scale model just enters into the smoke sheet

figure 10 b



1 wing span behind the model

figure 10 c



about 5 wing spans behind the model

FIGURE 10 : Example of smoke visualization

Afterwards, images recorded during the phenomenon are treated by software which gives the trajectory and velocity of each vortex centre.

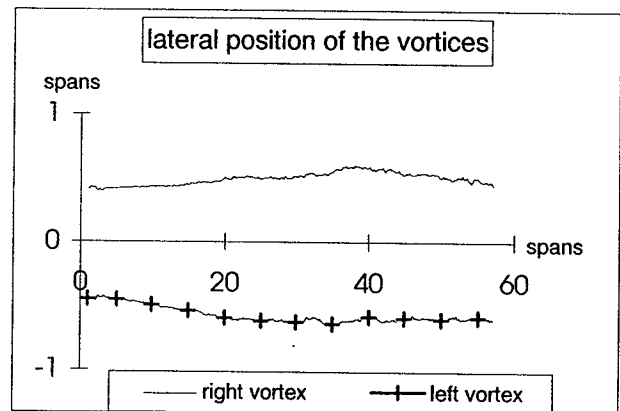
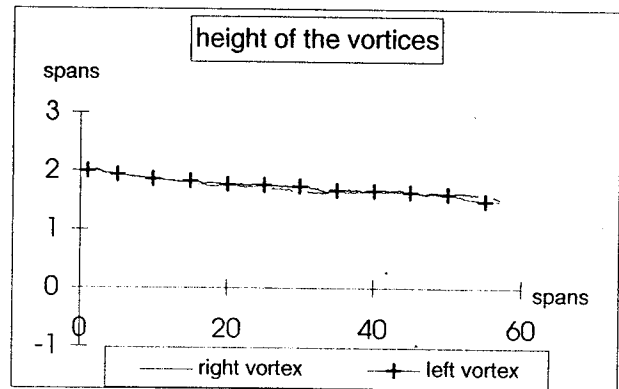


FIGURE 11 : Example of vortex trajectories

Tracking or P.I.V. measurements give information about the local velocities encountered in the flow field. This time the seeding of the observation area is made of soap bubbles filled with an air-helium mixture to obtain a density quite equal to that of the air. These bubbles are given out by a generator, equipped with two emitting heads, and a control desk to check the delivery of the different components. The diameter of the bubbles can be chosen in the interval [1 mm 10 mm] and the rate of bubble emission can be adjusted between 20 bubbles/s up to 500 bubbles/s.

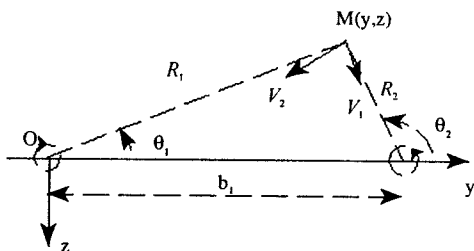
The main difficulty of this technique, when it is applied to model flight tests, is to obtain an homogeneous distribution of particles on a large observation area, when the seeding is made in steady air. Before the model goes through the plane, the particles must have no residual velocity and it is then necessary to stop the bubble emission during the observation interval. Afterwards, the bubbles are

carried away by the rotating movement of the vortices and that creates zones without any seeding, which are relatively large in this case.

As for the smoke visualizations, filming is by means of a black-and-white CCD video camera located under the catapult. The shooting frequency is equal to 50 frames (512 x 256 pixels) per second and the bubbles are lit with a white light by spotlights. In order to be able to follow the phenomenon during its whole evolution, the size of the observation area is 4 x 4 m or 2 x 2 m.

These techniques have enabled us to gather a preliminary data base and elaborate a formulation of velocities in the wake, which will be useful for flight mechanics applications. That means formulation with a relatively simple structure to enable, in particular, real time simulation. In its final form this formulation will be used to study behaviour of aircraft encountering a wake turbulence.

This formulation is :



$$R_1 = \sqrt{y^2 + z^2}$$

$$R_2 = \sqrt{(b_1 - y)^2 + z^2}$$

$$V_1 = \epsilon \left( 1 - \exp\left(-\frac{R_1^2}{\delta d}\right) \right) \frac{1}{R_1}$$

$$V_2 = \epsilon \left( 1 - \exp\left(-\frac{R_2^2}{\delta d}\right) \right) \frac{1}{R_2}$$

$$v = -V_1 \sin\theta_1 + V_2 \sin\theta_2$$

$$w = V_1 \cos\theta_1 - V_2 \cos\theta_2$$

$b_1$  is the distance between the two vortices and  $d$  is the separation distance between the leading aircraft, which generates the wake, and the following aircraft.  $\epsilon$  and  $\delta$  are identified from the data base.  $\epsilon$  depends on the leading aircraft wing circulation and  $\delta$  on the rate of vortex decay.

## Conclusion

As demonstrated by these applications, scale model flight tests provide an original contribution to study of environmental effects on aircraft flight.

This technique is complementary to wind tunnel tests and numerical methods. It gives access to non steady and transient aerodynamic effects and enables aerodynamic characterization of the whole aircraft or of parts of it. It provides data bases for physical modelling of the phenomena encountered.

This experimental technique is also used at ONERA/DCSD for studies of loss of control and start of spin and a second laboratory for catapulted model flight tests is devoted to these studies.

The flight domain, that is possible to study in these two laboratories, is restricted because of their dimensions imposed by the surface on the ground which was available when they were built. It is the reason why the project of a new facility is at present being investigated to make the best use of the experimental technique and be able to apply it to new fields of research.

In this new laboratory the observation area will be about 50m long, 20m wide and 21m high. Such dimensions will enable to perform tests with a high fall of level and a great yaw rate. This will be, in particular, interesting to experiment new control surface concepts, to validate control laws or to demonstrate certification criteria for spin and control loss resistance.

## References

- [1] Charon W., Verbrugge R. A., "Nouvelle technique d'essais sur maquettes libres en laboratoire pour la détermination de caractéristiques aérodynamiques" AGARD CP 235, 1978
- [2] Cocquerez J.-L., Coton P., Verbrugge R., "Etude de l'effet de sol sur maquette en vol" AGARD CP 465, 1989
- [3] Coton P., "Caractérisation et modélisation du sillage d'un avion de transport à partir d'essais en vol de maquettes en laboratoire" AGARD CP 584, 1996